Preparation and Properties of Plasticized Starch/ Multiwalled Carbon Nanotubes Composites

Xiaodong Cao,[1] Yun Chen,[1,2] Peter R. Chang,[1] Michel A. Huneault[3]

[1]*Bioproducts and Bioprocesses National Program, Agriculture and Agri-Food Canada, Saskatoon, Saskatchewan, Canada S7N 0X2*
[2]*Research Centre for Medicine, School of Medicine, Wuhan University, Wuhan 430071, China*
[3]*Industrial Materials Institute, National Research Council Canada, 75, de Mortagne, Boucherville, Québec, Canada J4B 6Y4*

Received 1 March 2007; accepted 29 May 2007
DOI 10.1002/app.26799
Published online 12 July 2007 in Wiley InterScience (www.interscience.wiley.com).

ABSTRACT: In this work we have studied the utilization of multiwalled carbon nanotubes (MWCNTs) as filler-reinforcement to improve the performance of plasticized starch (PS). The PS/MWCNTs nanocomposites were successfully prepared by a simple method of solution casting and evaporation. The morphology, thermal behavior, and mechanical properties of the films were investigated by means of scanning electron microscopy, wide-angle X-ray diffraction, differential scanning calorimetry, and tensile testing. The results indicated that the MWCNTs dispersed homogeneously in the PS matrix and formed strong hydrogen bonding with PS molecules. Compared with the pure PS, the tensile strength and Young's modulus of the nanocomposites were enhanced significantly from 2.85 to 4.73 MPa and from 20.74 to 39.18 MPa with an increase in MWCNTs content from 0 to 3.0 wt %, respectively. The value of elongation at break of the nanocomposites was higher than that of PS and reached a maximum value as the MWCNTs content was at 1.0 wt %. Besides the improvement of mechanical properties, the incorporation of MWCNTs into the PS matrix also led to a decrease of water sensitivity of the PS-based materials. © 2007 Wiley Periodicals, Inc. J Appl Polym Sci 106: 1431–1437, 2007

Key words: starch; thermoplastics; multiwalled carbon nanotubes; nanocomposite; reinforcement

INTRODUCTION

Advanced technology in the field of petrochemical-based polymers has brought many benefits to mankind. However, it is becoming more evident that the ecosystem is considerably disturbed and damaged as a result of the nondegradable plastic materials for disposable items. Thus, there is an urgent need to develop renewable source-based environmentally benign materials, which are novel materials of the 21st century and would be of great importance to the materials field, not only as a solution for growing environmental threats, but also as a solution for the uncertainty of the petroleum supply.[1,2] Among the many kinds of biodegradable polymers, starch is one of the most promising materials for biodegradable plastics because of its universality and low cost.[3,4] Thermoplastic starch (TPS) or plasticized starch (PS) can be made by incorporating plasticizers, such as water, glycerol, sorbitol, sugars, formamide, and other organics into starch.[5–10] PS has attracted considerable attention during the past decades and offers an interesting alternative for synthetic polymers where long-term durability is not needed and rapid degradation is desirable.[11,12] However, compared to conventional synthetic thermoplastics, biodegradable products based on starch, unfortunately, still exhibit many disadvantages, such as water sensitivity, poor processability, and poor mechanical properties.[13] To solve these problems, various physical or chemical modifications of the starch have been considered, including blending with other synthetic polymers,[14,15] the chemical modification,[16] or graft copolymerization,[17] and incorporating fillers such as lignin,[18] fibers or crystalline,[19–22] tunicin whiskers,[23,24] and clay.[25]

Multiwalled carbon nanotubes (MWCNTs) are stiff macromolecular structures having outer diameters of about 30 nm, and lengths of 1–100 μm.[26] The MWCNTs also have high modulus (1 TPa) along their length direction, as well as high bending modulus (0.9–1.24 TPa).[27] Therefore, they have been considered as ideal reinforcing fillers for polymer matrixes to achieve high performance and extensive applications since the discovery of carbon nanotube in 1991 by Iijima.[28–30] The most common methods, such as melt-blending and solution-casting, which are developed for making polymer composites with

Correspondence to: P. Chang (changp@agr.gc.ca).
Contract grant sponsor: Canadian Biomass Innovation Network (CBIN).

inorganic fillers, are also adopted for making MWCNTs-enhanced polymer composites.[31–34] It is well known that the effective utilization of MWCNTs in composite applications depends strongly on the ability to disperse the MWCNTs homogeneously throughout the matrix without destroying the integrity of the MWCNTs.[35] However, the nonreactive surface of MWCNTs usually limits their applications in composites because of a lack of adhesion between MWCNTs and polymer matrix. In the past decade, some efforts to improve dispersibility of MWCNTs have been explored, including the use of surfactants,[29] oxidation, or chemical functionalization of the MWCNTs surface.[36,37] For instance, introduction of carboxylic, carbonyl, and hydroxyl groups on MWCNTs by refluxing MWCNTs with nitric acid or mixed acid greatly enhanced their interaction with various polymer matrixes, thus improving the mechanical properties of the resulting composites.[38,39]

As Ratnayake et al.[40] reported, Canada is the largest producer (~ 25% of total world production) and the largest exporter (~ 40% of the total world exports) of field pea in the world. Pea starch and pea protein are the two main products from wet process in the pea industry. Because of a variety of applications, the market value for pea starch is relatively low and is affected by the market demand and supply from other sources. In this study, pea starch was used as a raw material to prepare PS matrix. The mixed acid treated MWCNTs were used as fillers to reinforce the PS matrix due to hydrogen bonding between the functionalized MWCNTs and PS matrix, the interfacial adhesion and mechanical performance of the composite are likely to be improved. A series of nanocomposite films of PS/MWCNTs with MWCNTs content ranged from 0.1 to 3.0 wt % were prepared by solution casting. The effects of MWCNTs content on the structure and properties of the nanocomposites were investigated by scanning electron microscopy (SEM), wide-angle X-ray diffraction (WAXD), differential scanning calorimetry (DSC), and testings of mechanical properties and water absorption.

EXPERIMENTAL

Materials

Field pea starch, with average granule size of about 29 μm and composed of 35% amylose and 65% amylopectin, was supplied by Nutri-Pea Limited Canada (Portage la Prairie, Canada). The plasticizer, glycerol (99% purity), was bought from Sigma–Aldrich Canada Ltd. (Oakville, Canada) and used as received. MWCNTs were also purchased from Sigma–Aldrich Canada Ltd. The MWCNTs were further functionalized as follows: 10 g of MWCNTs were added to a 200 mL mixture of concentrated sulfuric acid (98%) and nitric acid (60%) with volume 3 : 1. The mixture was ultrasonicated for 1 h, and then refluxed at 135°C for 2 h.[41,42] Subsequently, the resulting mixture was centrifuged and separated, and washed repeatedly with de-ionized water to neutrality. Then the solid was dried in vacuum at 60°C for 3 days, affording acid-treated MWCNTs of 6.94 g.

Preparation of the PS/MWCNTs nanocomposites films

The fabrication of PS/MWCNTs films was based on a convenient solution process. MWCNTs were dispersed in de-ionized water first and were homogenized in an ultrasonic bath for 30 min. Starch and glycerol were mixed and dispersed in distilled water. The mixture contained 6.4 wt % pea starch, 3.6 wt % glycerol, and 90.0 wt % water, respectively. Then it was charged into a round bottom flask equipped with stirrer and heated at 100°C for 20 min to be gelatinized. Subsequently, the desired weight of MWCNTs aqueous suspension was added and stirred for another 30 min. After degassing under vacuum and in an ultrasonic bath, the mixture was cast in a polystyrene Petri dish and dried in a ventilated oven at 50°C. By changing the concentration of MWCNTs to 0.1, 0.2, 0.5, 0.8, 1.0, 2.0, and 3.0 wt %, respectively, a series of PS/MWCNTs nanocomposite films with a thickness of around 0.3 mm were prepared and coded as PS-0.1, PS-0.2, PS-0.5, PS-0.8, PS-1.0, PS-2.0, and PS-3.0, in which the MWCNTs content was expressed on water-free PS matrix. As a control, a PS film without MWCNTs was obtained using the same fabrication process. Before various characterizations, the resulting films were kept in a conditioning desiccator of 43% relative humidity (RH) for more than one week at room temperature to ensure the equilibration of the water in the films.

Characterizations

The morphology of original and acid-treated MWCNTs was observed by a field emission scanning electron microscope (FESEM, JSM-6700F, Tokyo, Japan) at an acceleration voltage of 5 kV. And the fracture surfaces of the starch/MWCNTs composites were observed by a SEM (S-570, Hitachi, Ibaraki, Japan). The failure surfaces of the films after tensile testing were coated with gold and observed at 20 kV as accelerating voltage.

Wide-angle X-ray diffraction patterns were recorded on an X-ray diffraction instrument (XRD-6000, Shimadzu, Tokyo, Japan), using Cu Kα radiation ($\lambda = 0.154$ nm) at 40 kV and 30 mA with a scan

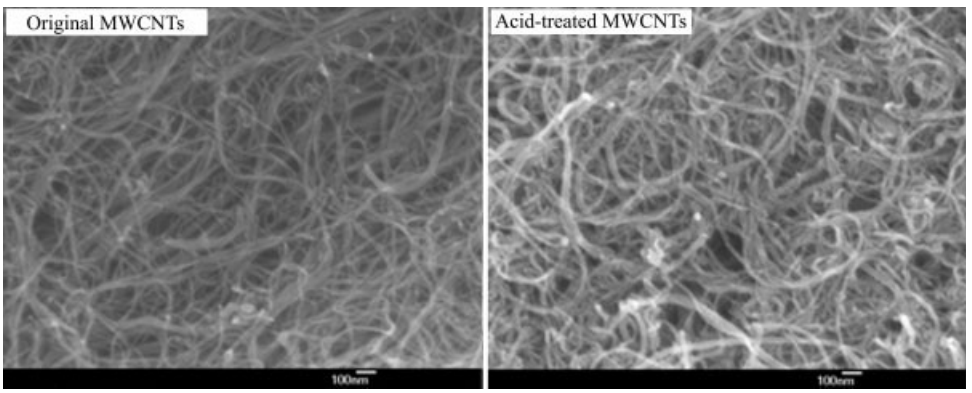

Figure 1 SEM images of the original and acid-treated MWCNTs.

rate of 4°/min. The diffraction angle ranged from 4 to 40°.

Differential scanning calorimetry (DSC) measurement of the films was carried out on a DSC200 PC apparatus (Netzsch Co., Selb, Germany) with cooling system using liquid nitrogen. Conditioned samples were placed in hermetic cells and two individual measurements were carried out to ensure the reliability. Each sample was heated from −100 to 250°C at a heating rate of 10°C/min. In this case, the glass transition temperature (T_g) was taken as the inflection point of the specific heat increment at the glass–rubber transition, and the melting temperature (T_m) was taken as the peak temperature of the melting endotherm. The heat of fusion (ΔH_m), calculated from the areas of the melting endotherm, was the ratio of the apparent enthalpy and of the weight fraction of the PS in the blends.

The mechanical properties of the films were measured on a universal testing machine (CMT 6503, Shenzhen SANS Test Machine Co., Shenzhen, China) at room temperature with gauge length of 5 cm and crosshead speed of 5 mm/min. An average value of five replicates for each sample was taken.

The moisture content of the PS/MWCNTs films was determined. The samples used were thin rectangular strips with dimension of 50 mm × 10 mm × 0.3 mm. They were vacuum-dried at 80°C overnight and then kept at 0% RH (P_2O_5) for one week. After weighting, they were conditioned at room temperature in a desiccator of 98% RH ($CuSO_4 \cdot 5H_2O$ saturated solution). The water uptake (WU) of the samples was calculated as follows:

$$\text{WU}\ (\%) = \frac{W_\infty - W_0}{W_0} \times 100 \qquad (1)$$

where W_0 and W_∞ were the weights of the sample before exposure to 98% RH and equilibrium weight, respectively. An average value of three replicates for each sample was taken.

RESULTS AND DISCUSSIONS

Morphology of the PS/MWCNTs nanocomposites

Figure 1 shows the SEM images of the original and acid-treated MWCNTs. The MWCNTs tangled together but can be identified. The diameter of the MWCNTs evaluated from SEM images was in the range of several nanometers to about 25 nm. No obvious differences in appearance and size between the original and acid-treated MWCNTs were observed.

Figure 2 shows the SEM images of the fracture surfaces for PS and PS/MWCNTs nanocomposite films after tensile testing. Some small cracks in the fracture surfaces resulted from the abrupt breaking during the tensile testing. Compared with the PS film, the morphology of the PS/MWCNTs can be easily identified. From the SEM images at relative lower magnification, no obvious large aggregates of MWCNTs are observed in the fracture surfaces when the MWCNTs content is lower than 1.0 wt %, suggesting that MWCNTs dispersed in PS matrix homogenously in this case. While at relatively higher MWCNTs contents (2.0 and 3.0 wt %), some MWCNTs ends on the failure of the PS/MWCNTs are observed clearly. It is worth noting that, upon failure, most of the MWCNTs were broken rather than just pulled out of the matrix. The ends of the broken MWCNTs at nanoscale can be obviously observed in the SEM images of PS-2.0 and PS-3.0 at the highest magnification in Figure 1. This phenomenon indicates a strong interfacial adhesion between the MWCNTs and the PS matrix. It has been proved that the acid-treatment process incorporated kinds of polar groups with MWCNTs, improved the hydrophilicity of MWCNTs, and reduced agglomerations of MWCNTs.[40] These are greatly contributed to enhance the hydrogen bonding interactions between acid-treated MWCNTs and PS, increase the compatibility between MWCNTs and PS, and result in an improvement of the mechanical performance of the PS/MWCNTs nanocomposite films as discussed later.

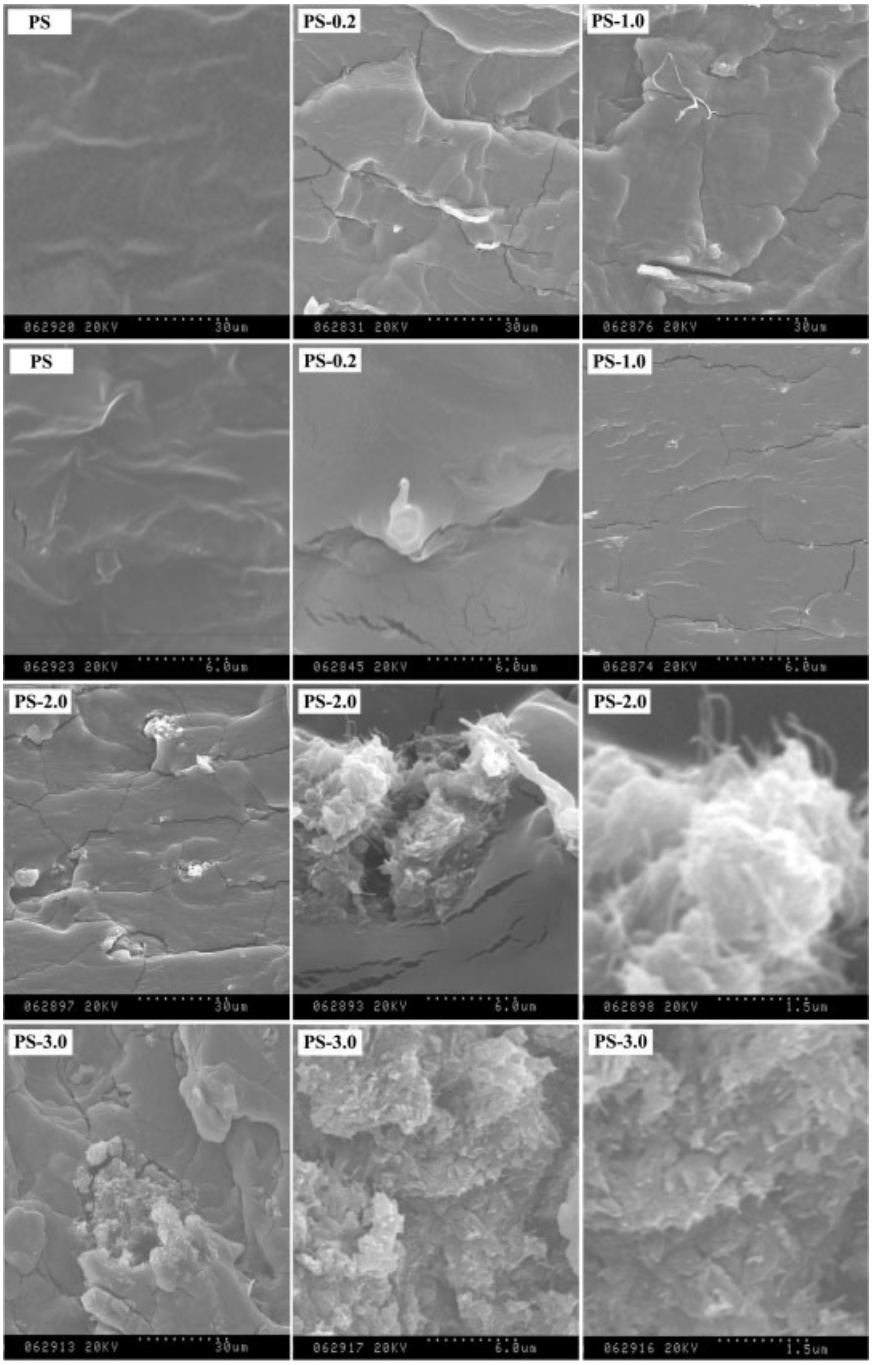

Figure 2 SEM images of the failure surfaces for PS and PS/MWCNTs nanocomposite films.

The nanocomposite materials resulting from the casting and evaporation were studied by WAXD as a function of the MWCNTs content and the corresponding diffractograms are shown in Figure 3. For PS film, the typical C-type crystallinity pattern with peaks at $2\theta = 5.6^\circ$ (characteristic of B type polymorphs), 15.0° (characteristic of A type polymorphs), 17.2° (characteristic of both A and B type polymorphs), 20.1° and 22.5° (characteristic of B type polymorphs) was observed clearly. The crystalline structure resulting from spontaneous recrystallization or retrogradation of starch molecules after melting or gelatinization has often been detected in food and in thermoplastic material.[43] The incorporation of MWCNTs did not have a significant effect on the crystalline structure of the PS matrix. The WAXD patterns of the PS/MWCNTs nanocomposites still retained characteristic peaks of pea starch regardless of the MWCNTs content. There is no evidence of any additional peak, such as an extra peak at $2\theta = 21.5^\circ$ ascribed to the accumulation of plasticizers at the interface of whiskers and starch is observed,

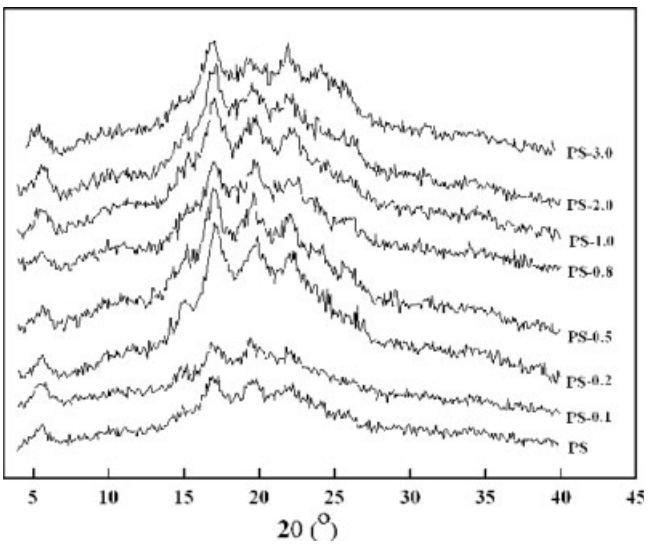

Figure 3 WAXD patterns of PS and PS/MWCNTs nanocomposites.

which was reported by Dufresne et al.[18] for glycerol PS based nanocomposites filled with whiskers. Therefore, it can be concluded that there is no transcrystallization in the MWCNTs reinforcing system.

Thermal properties

To further understand the structure and interaction between the two components, DSC studies of the PS and nanocomposites were performed. Figure 4 shows the DSC curves of PS matrix and nanocomposites reinforced with different MWCNTs content. Similar to the PS matrix, an endothermic peak at about 160°C attributed to the melting of starch crystallites for all nanocomposites was observed in all

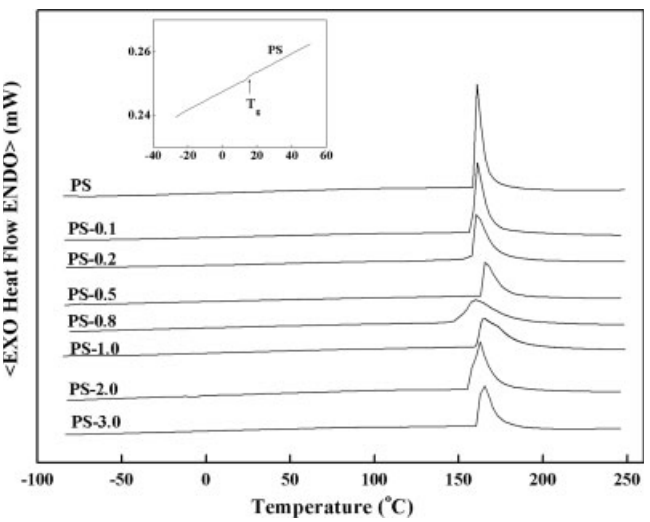

Figure 4 DSC curves of the PS and PS/MWCNTs nanocomposite films with different MWCNTs content.

curves regardless of the MWCNTs content. It demonstrates that the addition of MWCNTs in the PS matrix does not prohibit its retrogradation completely or change its crystallinity type, at least while MWCNTs content was lower than 3 wt %, which was in good agreement with the result from WAXD. However, it was observed that ΔH_m (Table I) decreases as the MWCNTs was incorporated. Generally, the retrogradation of PS is greatly dependent on the hydrogen bond-forming abilities of the additives with starch molecules. The stronger the hydrogen bond between starch and the additives, the more difficult for starch to re-crystallize during the storage period of PS. It demonstrates that the MWCNTs can form relative strong hydrogen bonding between PS and MWCNTs to suppress starch retrogradation, because of the carboxylic, carbonyl, and hydroxyl groups on acid-treated-MWCNTs. Especially, the composites with MWCNTs less than 1 wt% have a relatively lower value of ΔH_m, indicating the stronger interactions and better compatibility. Furthermore, there is no occurrence of shoulder peak on the melt endotherm of all DSC curves, indicating no new crystallinity in this case. Furthermore, there was no occurrence of shoulder peak on the melt endotherm of all DSC curves, indicating none of new crystallinity in this case. This is also supported by WAXD. In addition, a single ill-defined specific heat increment was observed at low temperature from all DSC curves, as shown in the insert for PS. It corresponded to the glass–rubber transition (T_g) of the PS matrix. The value of T_g for all the nanocomposites is also collected in Table I. As we know, the PS plasticized by glycerol exists as a complex heterogeneous system composed of glycerol-rich domains dispersed in a starch-rich continuous phase,[44] and each phase should exhibit its own T_g.[18] Therefore, the transition at 16.5°C of PS should be associated with glass transitions of starch-rich phase. The T_g transition of glycerol-rich phase located in the temperature region from −80 to −50°C, unfortunately, cannot be detected because of the low sensitivity of DSC. By incorporating MWCNTs fillers of 0–3 wt % into PS matrix, the T_g for starch-rich phase

TABLE I
The DSC Data of PS and the PS/MWCNTs Nanocomposites

Sample	T_g (°C)	ΔC_p (J g^{-1}K^{-1})	T_m (°C)	ΔH_m (J g^{-1})
PS	16.5	0.042	160.8	17.4
PS-0.1	16.7	0.036	160.6	14.6
PS-0.2	17.2	0.039	160.9	9.5
PS-0.5	20.2	0.034	166.0	8.9
PS-0.8	19.8	0.038	158.0	12.6
PS-1.0	22.5	0.031	165.1	11.6
PS-2.0	24.1	0.045	159.7	15.9
PS-3.0	25.3	0.041	160.9	15.4

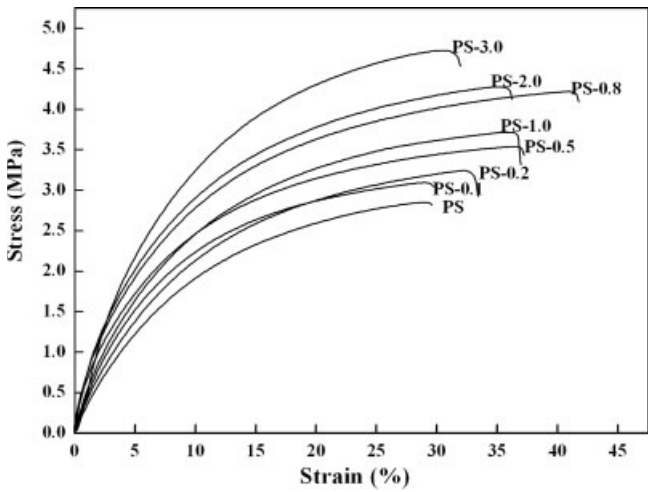

Figure 5 Stress–strain curves of PS and PS/MWCNTs nanocomposite films with different MWCNTs content.

shifts to higher temperature from 16.5 to 25.3°C. The dependence of T_g on the content of MWCNTs might be attributed to the occurrence of intermolecular interactions between starch and stiff MWCNTs, which reduced the flexibility of molecular chains of starch in contact with the MWCNTs surface.

Mechanical properties

The typical stress–strain curves of the PS and its MWCNTs nanocomposites are shown in Figure 5. The corresponding tensile properties are summarized in Table II. The MWCNTs content has a profound effect on the tensile properties. It was evident that even the presence of a small amount of MWCNTs would largely improve the tensile properties. The tensile strength and Young's modulus increased significantly from 2.85 to 4.73 MPa and from 20.74 to 39.18 MPa with an increase of MWCNTs content from 0 to 3.0 wt %, respectively. It was worth noting that the increase in strength did not come at the expense of the elongation at break, which exists in conventional filled polymer systems.

TABLE II
Mechanical Properties of the PS and PS/MWCNTs Nanocomposite Films Obtained from Tensile Testing

Samples	σ_b (MPa)	ε_b (%)	E (MPa)
PS	2.85 ± 0.32	29.69 ± 3.21	20.74 ± 1.23
PS-0.1	3.04 ± 0.21	29.70 ± 2.01	24.20 ± 2.36
PS-0.2	3.17 ± 0.19	33.18 ± 3.02	24.54 ± 1.56
PS-0.5	3.54 ± 0.25	37.22 ± 2.36	24.81 ± 2.30
PS-0.8	3.72 ± 0.34	36.93 ± 3.81	26.58 ± 1.89
PS-1.0	4.10 ± 0.37	41.99 ± 2.10	27.83 ± 2.01
PS-2.0	4.29 ± 0.30	38.29 ± 3.12	31.51 ± 2.56
PS-3.0	4.73 ± 0.14	32.03 ± 1.20	39.18 ± 1.43

σ_b, tensile strength; E, Young's modulus; ε_b, elongation at break.

From Table II, we can see the values of elongation at break getting increased with an increase of MWCNTs content in the range of 0–1.0 wt %. The maximum value was reached at 41.99% for the sample with 1.0 wt % MWCNTs. Both the tensile strength and Young's modulus are 4.10 and 27.83 MPa, increased by 42 and 34%, respectively, compared with those of PS. When the MWCNTs content was higher than 1.0%, the elongation at break of PS/MWCNTs films decreased slightly, but still was higher than that of PS. This may be attributed to some degree of aggregations of the MWCNTs.[45] Generally, the results from tensile testing indicate that the mechanical properties of the PS/MWCNTs nanocomposites are better than those of neat PS. This probably can be explained by the reinforcement effect from the homogeneously dispersed high-performance MWCNTs fillers in the PS matrix and strong hydrogen bonding interaction between MWCNTs and PS molecules. Therefore, the compatibility of MWCNTs and starch was enhanced as a result of the homogeneous dispersion of MWCNTs and the strong interfacial adhesion between MWCNTs and starch, which improved the mechanical properties of the composites.

Water absorption

As one of the major drawbacks in the use of starch systems is their water absorption tendency, any improvement in water resistance is highly important. The water uptake at equilibrium of the PS and PS/MWCNTs films with different MWCNTs content at a relative humidity of 98% are plotted in Figure 6. It was observed that the unfilled PS absorbed around

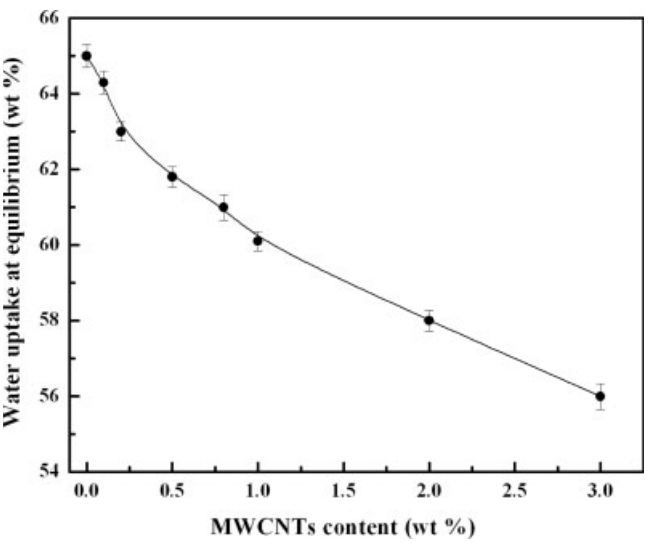

Figure 6 Water uptake at equilibrium of the PS and PS/MWCNTs films conditioned at 98% RH as a function of MWCNTs content.

65 wt % of water. The water uptake at equilibrium decreased as the MWCNTs content increased, and it was only about 56 wt % for the PS-3.0. Therefore, the swelling of the PS matrix reduced in the presence of MWCNTs in the nanocomposites. This phenomenon can be ascribed to the presence of strong hydrogen bonding interactions between MWCNTs and starch matrix. The hydrogen bonding interactions in the nanocomposites tended to suppress the swelling of the starch matrix when submitted to highly moist atmospheres. Meanwhile, the relatively low water sensitivity of MWCNTs and low glycerol content to whole material might also be responsible for the reduction of the water uptake at equilibrium.

CONCLUSIONS

Nanocomposites were prepared from glycerol plasticized pea starch as the matrix and acid-treated MWCNTs as reinforcing fillers. The SEM micrograph showed a very good dispersion of MWCNTs in the matrix and a strong adhesion between the matrix and MWCNTs. The values of T_g ascribed to the starch-rich phase increased with an increase of MWCNTs content, indicating that the MWCNTs were compatible with PS matrix and reduced the flexibility of starch molecular chains. Compared with the unfilled PS, the tensile strength and Young's modulus of the nanocomposites increased, respectively, from 2.85 to 4.73 MPa and from 20.74 to 39.18 MPa with an increase of MWCNTs content from 0 to 3.0 wt %. It is worth noting that the values of elongation at break of PS/MWCNTs nanocomposites were all higher than that of PS, and reached a maximum value as the MWCNTs content was 1.0 wt %. The presence of MWCNTs also decreased the water uptake at moisture equilibrium of the nanocomposites. The improvement of the properties of the PS/MWCNTs may be ascribed to the strong hydrogen bonding between MWCNTs fillers and PS matrix.

References

1. Mohanty, A. K.; Misra, M.; Drzal, L. T. J Polym Environ 2002, 10, 19.
2. Cakmakli, B.; Hazer, B.; Tekin, I. O.; Kizgut, S.; Koksal, M.; Menceloglu, Y. Macromol Biosci 2004, 4, 649.
3. Choi, E. J.; Kim, C. H.; Park, J. K. J Polym Sci Part B: Polym Phys 1999, 37, 2430.
4. Mohanty, A. K.; Misra, M.; Hinrichsen, G. Macromol Mater Eng 2000, 276/277, 1.
5. Carvalho, A. J. F.; Job, A. E.; Alves, N.; Curvelo, A. A. S.; Gandini, A. Carbohydr Polym 2003, 53, 95.
6. Gaudin, S.; Lourdin, D.; Forssell, P. M.; Colonna, P. Carbohydr Polym 2000, 43, 33.
7. Talja, R. A.; Helén, H.; Roos, Y. H.; Jouppil K. Carbohydr Polym 2007, 67, 288.
8. Rodriguez-Gonzalez, F. J.; Ramsay, B. A.; Favis, B. D. Carbohydr Polym 2004, 58, 139.
9. Da Róz, A. L.; Carvalho, A. J. F.; Gandini, A.; Curvelo, A. A. S. Carbohydr Polym 2006, 63, 417.
10. Yang, J. H.; Yu, J. G.; Feng, Y. Ma, X. F. Carbohydr Polym 2007, 69, 256.
11. Van Soest, J. J. G.; Benes, K.; DeWit, D.; Vliegenthart, J. F. G. Polymer 1996, 37, 3543.
12. Dintcheva, N. T.; La Mantia, F. P. Polym Degrad Stab 2007, 92, 630.
13. Santayanon, R.; Wootthikanokkhan, J. Carbohydr Polym 2003, 51, 17.
14. Dufresne, A.; Vignon, M. R. Macromolecules 1998, 31, 2693.
15. Huneault, M. A.; Li, H. Polymer 2007, 48, 270.
16. Sagar, A. D.; Merrill, E. W. J Appl Polym Sci 1995, 58, 1647.
17. Suda, K.; Kanlaya, M.; Manit, S. Polymer 2002, 43, 3915.
18. Lepifre, S.; Froment, M.; Cazaux, F.; Houot, S.; Lourdin, D.; Coqueret, X.; Lapierre, C.; Baumberger, S. Biomacromolecules 2004, 5, 1678.
19. De Carvalho, A. J. F.; Curvelo, A. A. S.; Agnelli, J. A. M. Int J Polym Mater 2002, 51, 647.
20. Soykeabkaew, N.; Supaphol, P.; Rujiravanit, R. Carbohydr Polym 2004, 58, 53.
21. Lu, Y.; Weng, L.; Cao, X. Carbohydr Polym 2005, 63, 198.
22. Lu, Y.; Weng, L.; Cao, X. Macromol Biosci 2005, 5, 1101.
23. Angles, M. N.; Dufresne, A. Macromolecules 2000, 33, 8344.
24. Mathew, A. P.; Dufresne, A. Biomacromolecules 2002, 3, 609.
25. Chen, B.; Evans, J. R. G. Carbohydr Polym 2005, 61, 455.
26. Ajayan, P. M. Chem Rev 2002, 99, 1787.
27. Qi, H. J.; Teo, K. B. K.; Lau, K. K. S.; Boyce, M. C.; Miline, W. I.; Robertson, J.; Gleason, K. K. J Mech Phys Solids 2003, 51, 2213.
28. Iijima, S. Nature 1991, 354, 56.
29. Hughes, M.; Chen, G. Z.; Shaffer, M. S. P.; Fray, D. J.; Windle, A. H. Chem Mater 2002, 14, 1610.
30. Ajayan, P. M.; Stephan, O.; Colliex, C.; Trauth, D. Science 1994, 265, 1212.
31. Shaffer, M. S. P.; Windle, A. H. Adv Mater 1999, 11, 937.
32. Pirlot, C.; Willems, I.; Fonseca, A.; Nagy, J. B.; Delhalle, J. Adv Eng Mater 2002, 4, 109.
33. Potschke, P.; Fornes, T. D.; Paul, D. R. Polymer 2002, 43, 3247.
34. Liu, T. X.; Phang, I. Y.; Shen, L.; Chow, S. Y.; Zhang, W. D. Macromolecules 2004, 37, 7214.
35. Ruan, S. L.; Gao, P.; Yang, X. G.; Yu, T. X. Polymer 2003, 44, 5643.
36. Thostenson, E. T.; Chou, T. W. J Phys D: Appl Phys 2002, 35, 77.
37. Huang, H. M.; Liu, I. C.; Chang, C. Y.; Tsai, H. C.; Hsu, C. H.; Tsiang, R. C. C. J Polym Sci Part A: Polym Chem 2004, 42, 5802.
38. Wang, S.; Shen, L.; Zhang, W.; Tong, Y. Biomacromolecules 2005, 6, 3067.
39. Kwon, J.; Kim, H. J Polym Sci Part A: Polym Chem 2005, 43, 3973.
40. Ratnayake, W. S.; Hoovar, R.; Warkentin, T. Starch/Stärch 2002, 54, 217.
41. Gao, C.; Vo, C. D.; Jin, Y. Z.; Li, W. W.; Armes, S. P. Macromolecules 2005, 38, 8634.
42. Liu, J.; Rinzler, A. G.; Dai, H. J.; Hafner, J. H.; Bradley, R. K.; Boul, P. J.; Lu, A.; Lverson, T.; Shelimov, K.; Huffiman, C. B.; Rodriguez-Macias, F.; Shon, Y. S.; Lee, T. R.; Colbert, D. T.; Smalley, R. E. Science 1998, 280, 1253.
43. Souza Rosa, R. C. R.; Andrade, C. T. J Appl Polym Sci 2004, 92, 2706.
44. Averous, L.; Boquillon, N. Carbohydr Polym 2004, 56, 111.
45. Lee, H.; Lin, L. Macromolecules 2006, 39, 6133.